Draft version May 14, 2023
Typeset using LaTeX **twocolumn** style in AASTeX631

# SN 2022joj

Chang Liu [1,2] Adam A. Miller [1,2] and Friends

[1] *Department of Physics and Astronomy, Northwestern University, 2145 Sheridan Rd, Evanston, IL 60208, USA*
[2] *Center for Interdisciplinary Exploration and Research in Astrophysics (CIERA), Northwestern University, 1800 Sherman Ave, Evanston, IL 60201, USA*

## ABSTRACT

*Keywords:* Supernovae (1668), Type Ia supernovae (1728), White dwarf stars (1799), Observational astronomy (1145), Surveys (1671)

## 1. INTRODUCTION

## 2. OBSERVATIONS

### 2.1. *Optical Photometry*

### 2.2. *Optical Spectroscopy*

**Table 1.** Spectroscopic observations of SN 2022joj and the host galaxy.

| $t_{\rm obs}$ (MJD) | Phase (days) | Telescope/ Instrument | $R$ ($\lambda/\Delta\lambda$) | Range (Å) |
|---|---|---|---|---|
| 59,710.29 | −12.5 | LCO/FLOYDS-N | 400–700 | 3500–10000 |
| 59,725.34 | +2.2 | P60/SEDM | 100 | 3770–9220 |
| 59,725.43 | +2.2 | P60/SEDM | 100 | 3770–9220 |
| 59,732.02 | +8.7 | NOT/ALFOSC | 360 | 3500–9700 |
| 59,744.96 | +21.3 | LT/SPRAT | 350 | 4020–7990 |
| 59,752.50 | +28.6 | LCO/FLOYDS-S | 400–700 | 3500–10000 |
| 59,759.92 | +35.8 | LT/SPRAT | 350 | 4020–7990 |
| 59,760.37 | +36.3 | Keck I/LRIS | 1100 | 3100–10280 |
| 59,784.89 | +60.1 | NOT/ALFOSC | 360 | 3850–9620 |
| 60,017.42 | +286.5 | MMT/Binospec | 1340 | 3830–9210 |
| 60,061.56 | +329.4 | Keck I/LRIS | 1100 | 3200–10150 |

Note—Phase is measured relative to the $r_{\rm ZTF}$-band peak in the rest frame of the host galaxy. The resolution $R$ is reported for the central region of the spectrum.

## 3. ANALYSIS

### 3.1. *Optical Spectral Properties*

## 4. DISCUSSION

### 4.1. *Models*

### 4.2. *Nebular-phase Spectra*

- weak emission in the 7300 complex compared to normal SNe Ia – similar to 91T-like events
- Blueshifted [Fe II] 7300 features ($\sim -2.21 \pm 0.33\,{\rm km\,s^{-1}}$ in the Binospec spectrum; $\sim -1.24 \pm 0.42\,{\rm km\,s^{-1}}$ in the LRIS spectrum), consistent with low-Si II-velocity SNe Ia
- No evidence for [Ni II] $\lambda\lambda$7378, 7412 or [Ca II] $\lambda\lambda$7291, 7323 – 3-$\sigma$ upper limit for $M_{\rm Fe}/M_{\rm Ni}$ is 0.05 (techniques adopted from Maguire et al. (2018)), consistent with sub-$M_{\rm Ch}$ DDet scenario?

## 5. CONCLUSIONS

*Facility:* PO:1.2m (ZTF), PO:1.5m (SEDM), FTN (FLOYDS), FTS (FLOYDS), NOT (ALFOSC), Liverpool:2m (SPRAT), Keck:I (LRIS), MMT (Binospec).

*Software:* `astropy` (Astropy Collaboration et al. 2013, 2018), `CASTRO` (Almgren et al. 2010), `dynesty` (Speagle 2020), `LAMBDAR` (Wright 2016), `matplotlib` (Hunter 2007), `prospector` (Johnson et al. 2021), `PypeIt` (Prochaska et al. 2020), `pysedm` (Rigault et al. 2019), `Python-FSPS` (Conroy et al. 2009; Conroy & Gunn 2010), `scipy` (Virtanen et al. 2020), `seaborn` (Waskom 2021), `SEDONA` (Kasen et al. 2006).

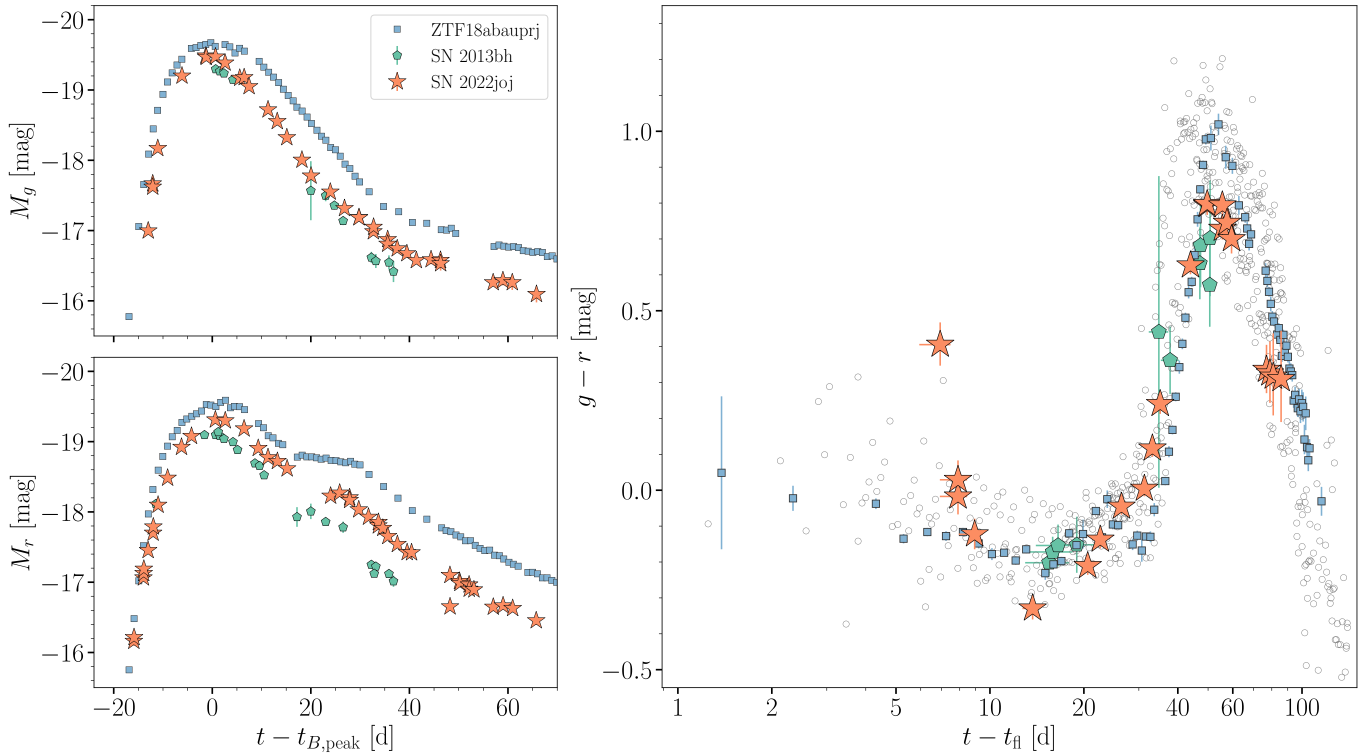


**Figure 1.** Comparison of the photometric properties of SN 2022joj with those of ZTF18abauprj (99aa-/91T-like SN) and SN 2013bh (00cx-like SN). *Left*: multiband light curves. The upper (lower) panel shows the evolution in the $g$-band ($r$-band) absolute magnitude. *Right*: $g-r$ color evolution. The gray circles denote the $g_{\mathrm{ZTF}} - r_{\mathrm{ZTF}}$ color evolution of 12 nearby ($z \leq 0.05$) normal SNe Ia (open circles) from the ZTF sample with prompt observations within 5 days of first light (Bulla et al. 2020).

## REFERENCES


Almgren, A. S., Beckner, V. E., Bell, J. B., et al. 2010, ApJ, 715, 1221, doi: 10.1088/0004-637X/715/2/1221

Astropy Collaboration, Robitaille, T. P., Tollerud, E. J., et al. 2013, A&A, 558, A33, doi: 10.1051/0004-6361/201322068

Astropy Collaboration, Price-Whelan, A. M., Sipőcz, B. M., et al. 2018, AJ, 156, 123, doi: 10.3847/1538-3881/aabc4f

Bulla, M., Miller, A. A., Yao, Y., et al. 2020, ApJ, 902, 48, doi: 10.3847/1538-4357/abb13c

Conroy, C., & Gunn, J. E. 2010, ApJ, 712, 833, doi: 10.1088/0004-637X/712/2/833

Conroy, C., Gunn, J. E., & White, M. 2009, ApJ, 699, 486, doi: 10.1088/0004-637X/699/1/486

Hunter, J. D. 2007, Computing in Science and Engineering, 9, 90, doi: 10.1109/MCSE.2007.55

Johnson, B. D., Leja, J., Conroy, C., & Speagle, J. S. 2021, ApJS, 254, 22, doi: 10.3847/1538-4365/abef67

Kasen, D., Thomas, R. C., & Nugent, P. 2006, ApJ, 651, 366, doi: 10.1086/506190

Maguire, K., Sim, S. A., Shingles, L., et al. 2018, MNRAS, 477, 3567, doi: 10.1093/mnras/sty820

Prochaska, J. X., Hennawi, J., Cooke, R., et al. 2020, pypeit/PypeIt: Release 1.0.0, v1.0.0, Zenodo, doi: 10.5281/zenodo.3743493

Rigault, M., Neill, J. D., Blagorodnova, N., et al. 2019, A&A, 627, A115, doi: 10.1051/0004-6361/201935344

Speagle, J. S. 2020, MNRAS, 493, 3132, doi: 10.1093/mnras/staa278

Virtanen, P., Gommers, R., Oliphant, T. E., et al. 2020, Nature Methods, 17, 261, doi: 10.1038/s41592-019-0686-2

Waskom, M. L. 2021, Journal of Open Source Software, 6, 3021, doi: 10.21105/joss.03021

Wright, A. H. 2016, LAMBDAR: Lambda Adaptive Multi-Band Deblending Algorithm in R, Astrophysics Source Code Library, record ascl:1604.003. http://ascl.net/1604.003

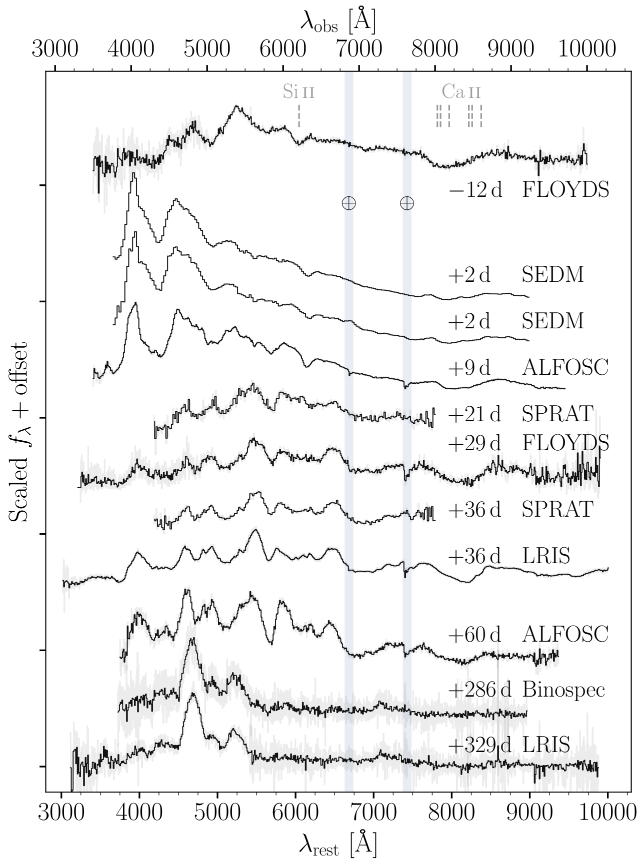


**Figure 2.** Optical spectral sequence of SN 2022joj. Rest-frame phases (days) relative to the $B$-band peak and instruments used are posted next to each spectrum. Spectra have been corrected for $E(B-V)_{\rm MW} = 0.04$ mag and are shown in gray. The black lines are binned spectra with a bin size of 10 Å, except for the SEDM spectra, whose resolution is lower than the bin size. The corresponding wavelengths of the Si II $\lambda$6355 line (with an expansion velocity of 10,000 km s$^{-1}$) and the Ca II IRT (with expansion velocities of both 10,000 km s$^{-1}$and 25,000 km s$^{-1}$) are marked by the vertical dashed lines.

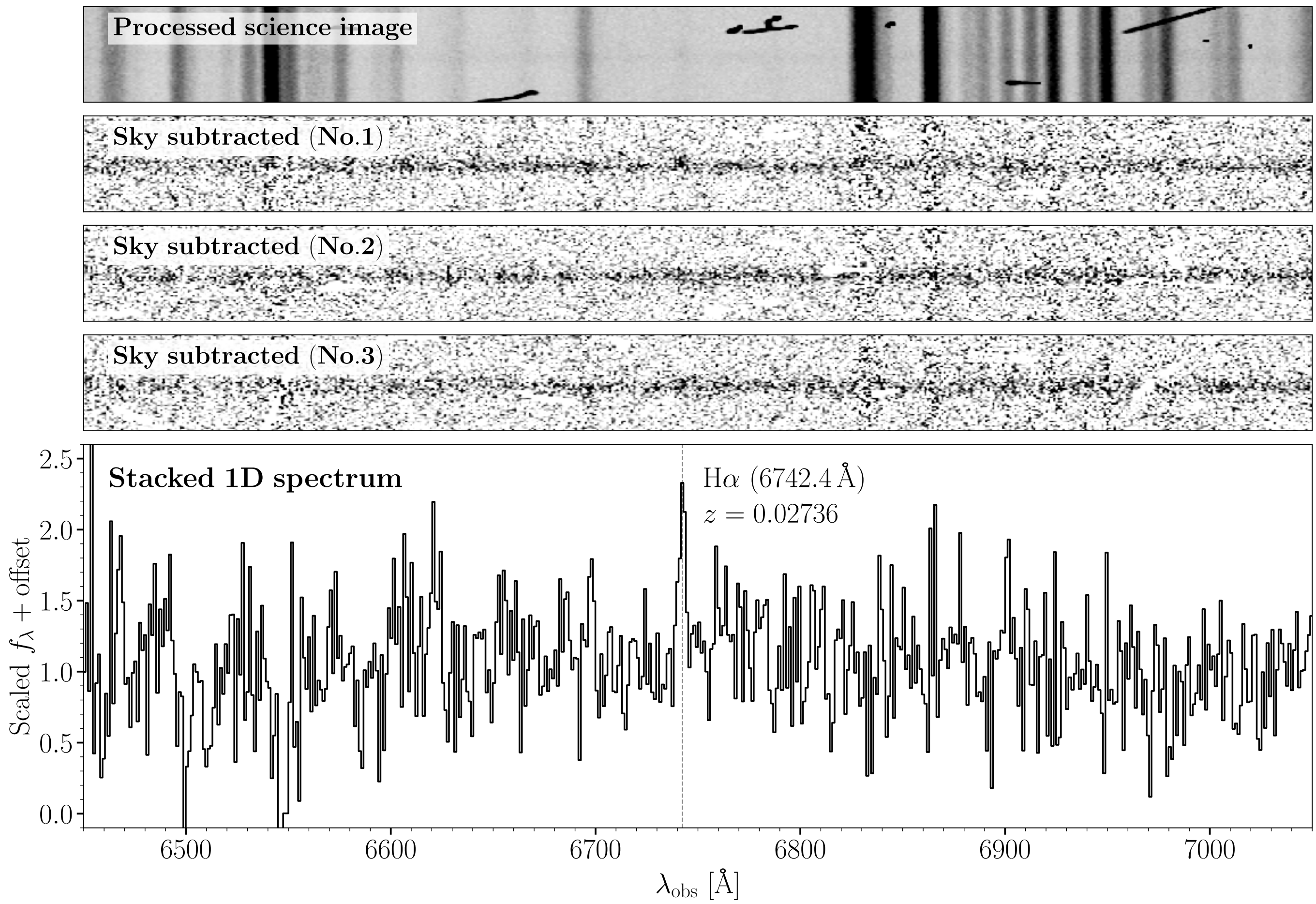


**Figure 3.** The LRIS spectra reveal the H$\alpha$ emission line from the host galaxy at 6742.4 Å, corresponding to a redshift $z = 0.02736$.

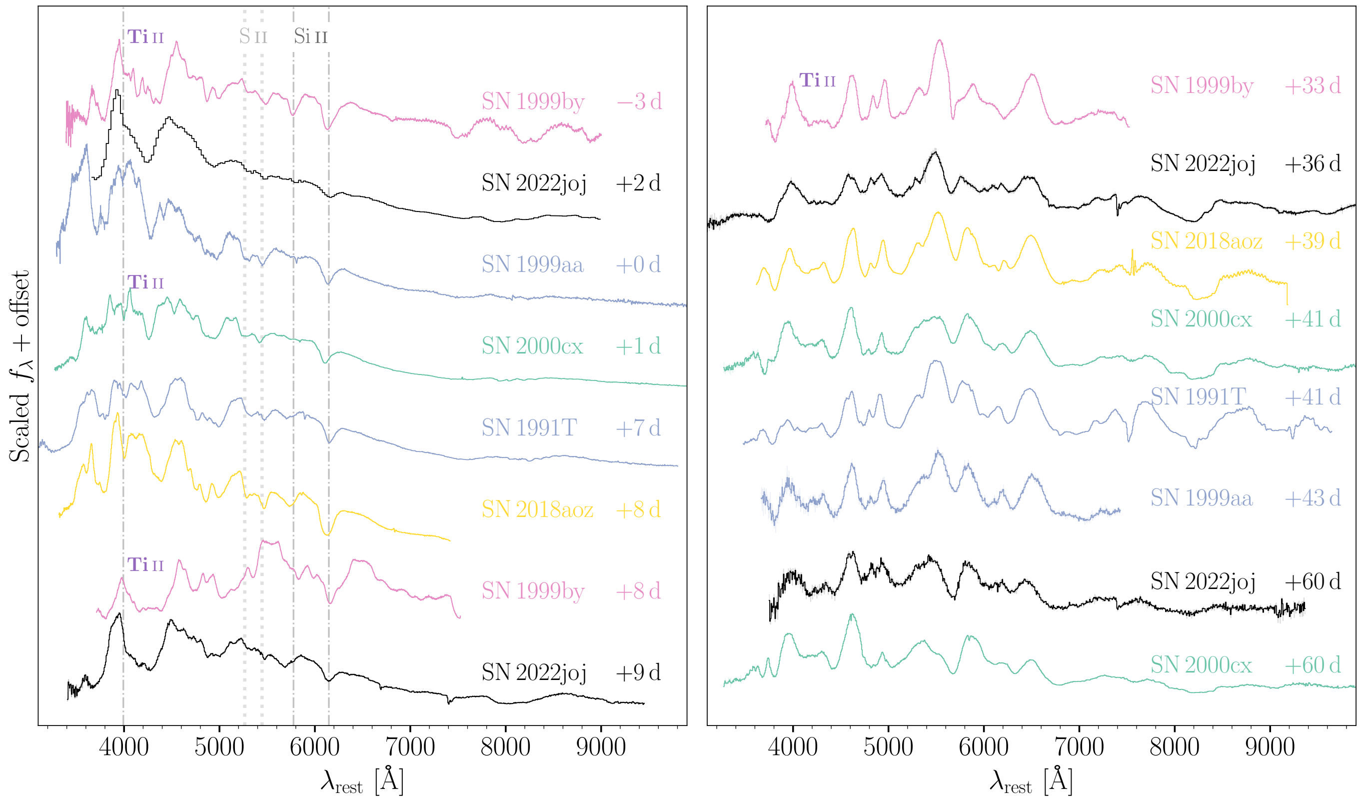


**Figure 4.** Optical spectral sequence of SN 2022joj.

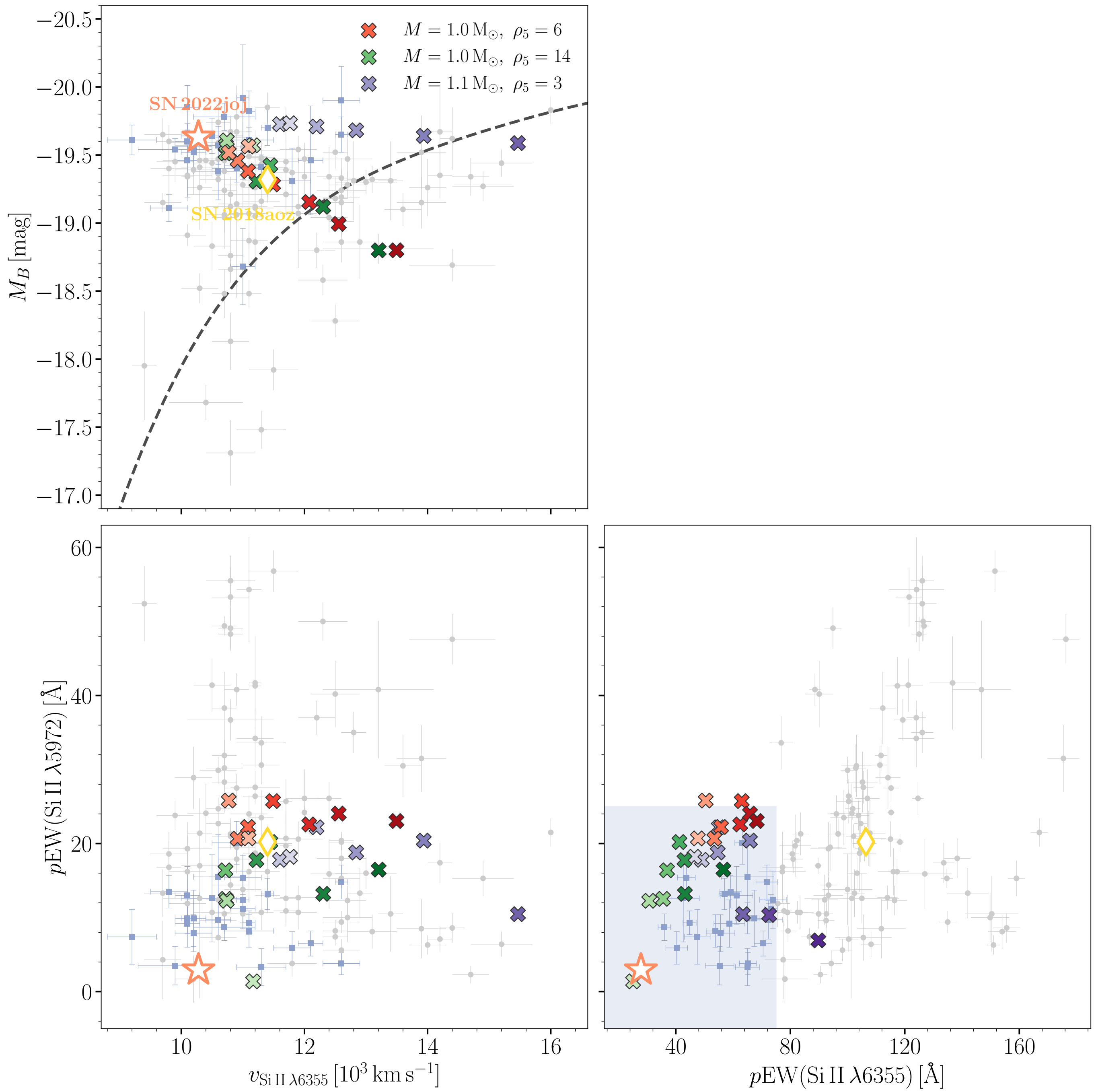


**Figure 5.** SN 2022joj as a SN Ia in the shallow-silicon class.

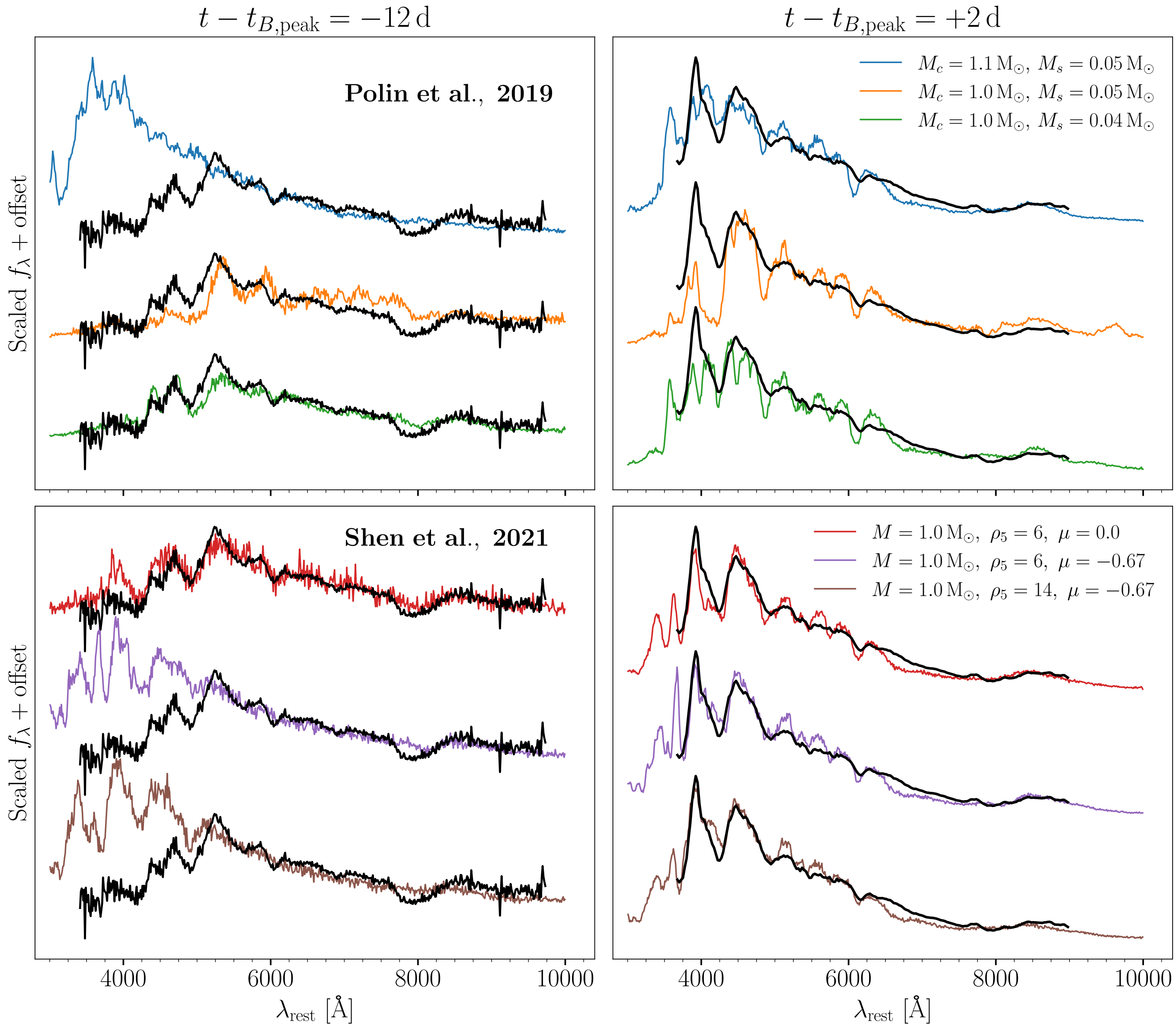


**Figure 6.** SN 2022joj v.s. DDet models.